International Research Journal of
SCIENCE, TECHNOLOGY, EDUCATION, AND MANAGEMENT
P-ISSN: 2799-063X | E-ISSN: 2799-0648
ISO 9001:2015 certified
Volume 3, No. 4 | December 2023

# Investigation on performance analysis of pyramid solar water distillation system

**Sabae Khaing[1], War War Min Swe[2]**
[1]*Mandalay Technological University, Myanmar*
[2]*Mandalay Technological University, Myanmar*
Corresponding email: khaingsabae87@gmail.com

## ABSTRACT

Solar water distillation systems are required for developing countries, especially in rural areas with an increasing population and environmental water pollution where there is no clean drinking water. Thus, solar still is the most important technology to increase pure water productivity in these regions. So, it is necessary to explore more about the system of solar distillation. In practical applications, design and performance analysis are essential to predict the efficiency of the solar still. This study aims to present the analysis of the temperature profile and fresh water output of the pyramid-shaped solar water distillation system by theoretical, numerical, and experimental analysis. The CFD simulation of the solar water distillation system was created using ANSYS FLUENT, and the experimental test was conducted in Mandalay, Myanmar, which is situated at a North Latitude of 21.996° and an East Longitude of 96.1° on 23rd April, 2022. In the performance analysis, the glass cover was tilted at 45°, and the water depth in the basin was 1 cm. For output verification, the experimental measurements were compared with theoretical and numerical results. The highest solar heat flux was 811.36 W/m$^2$ in theory and 799.32W/m$^2$ in experiment at 12:00 noon. During the solar still operation, the basin temperature was higher than the water and glass cover temperatures. The highest operating temperatures in the solar still in theoretical, numerical, and experimental analysis were 330 K, 331 K and 332 K respectively. The maximum pure water productivity was obtained at 335.5 ml/hr in theoretical analysis, 357.4 ml/hr in numerical analysis, and 437.5 ml/hr in experimental analysis. It has been found that all the analytical results among the theoretical, numerical, and experimental works show good agreement, which verifies and supports each other.

## ARTICLE INFO

Received : Nov. 11, 2023
Revised : Nov. 30, 2023
Accepted : Dec. 30, 2023

## KEYWORDS

*Pyramid solar still, Performance, Productivity, Solar energy, Temperature profile*

**Suggested Citation (APA Style 7th Edition):**

Khaing, S. & Swe, W.W.M. (2023). Investigation on performance analysis of pyramid solar water distillation system. *International Research Journal of Science, Technology, Education, and Management*, 3(4), 73-91. https://doi.org/10.5281/zenodo.10516210

## INTRODUCTION

Nowadays, fresh and clean water are very important in our society. In the future, everyone must receive drinking water. For this reason, it is to reduce water pollution and the proportion of raw sewage, and to increase recovery and safe clean water globally. The process of producing fresh and clean water from wastewater and/or untreated water (e.g., sea water, salt water, tap water) becomes important for domestic, hospital, and industrial applications. Solar energy-based distillation has become a popular way to produce fresh water with naturally harvested solar energy, especially in rural areas and remote villages where there is no electricity. Therefore, exploring many different ways of producing fresh water has become an essential topic in science and engineering.

The working principle of solar water distillation is established by the evaporation and condensation of working water. Figure.1 shows a model solar still. It mainly consists of a painted basin (absorber) that stores tap water or untreated waste water, a glass cover that serves as an absorbent of solar energy, a distilled trough channel that is to be used to collect the condensed water, a piping system, and buckets that are to collect the distilled water from the beaker. If there is no extra solar energy for pre-heating in a water distillation system, it is called a passive system, and if pre-heating is applied, it is called an active system.

Actually, the main performance of a solar energy-based water distillation system can be measured by the amount of fresh water produced in a given period of time. The efficiency of a solar energy-based water distillation system depends on many parameters, such as the amount of heat collected, the weather conditions, the level of the water depth in the basin, the absorber color, the location of the system, the shape and size of the collector cover, the inheritance of the working fluid, and the orientation of the system, as well as the supply of extra energy.

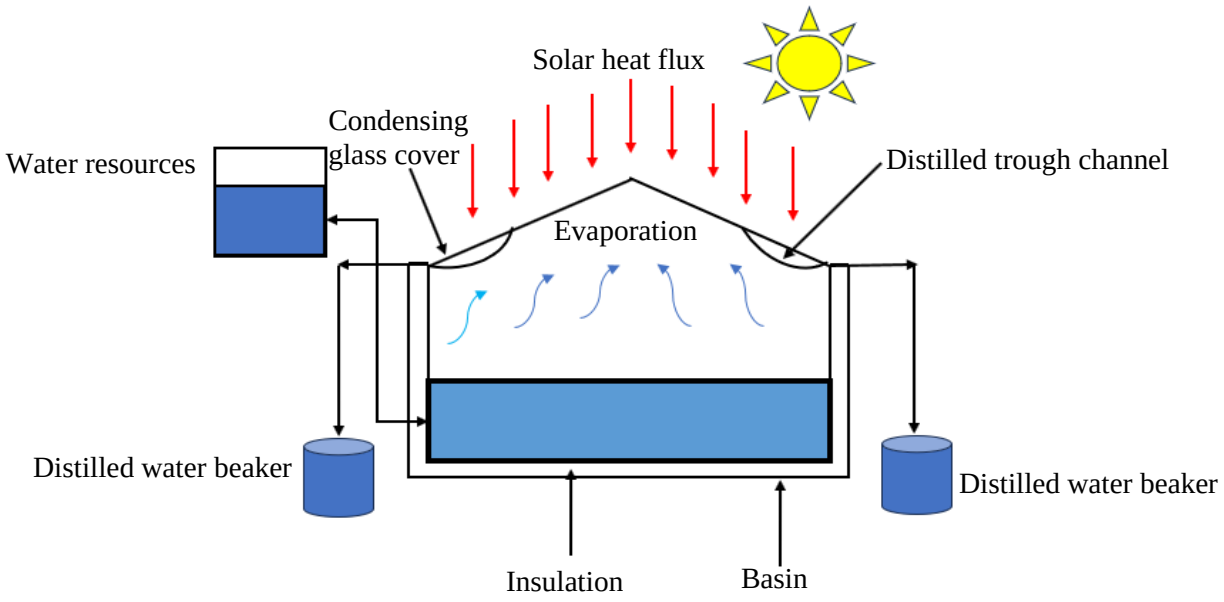


Figure 1. Typical model of pyramid type solar still

Among these factors, the most important thing is the glass cover (collector cover), which serves two functions: collecting solar energy and condensing the surface of the cover. The system design shape, size, and tilted angle of the glass cover significantly affect the efficiency of the system. Therefore, there have been many studies on the efficiency of solar distillation systems with respect to some factors: design parameters, climate parameters, and operation parameters.

In some previous works (Al-Garni et al., 2011; Sing, 2013), the effects of glass cover inclination were studied. The inclination angle was changed to 15°, 25°, 30°, 35°, 40°, and 45°. One common observation from these works was that a higher inclination angle can give a larger yield of fresh water. The optimum inclination angle should be between

30° and 45° (Garni et al., 2011; Sing, 2013). These (Al-Garni et al., 2011; Sonker, V.K. et al., 2019) investigated how water level affects solar still performance. These authors stated that the larger the glass cover thickness, the lower the performance of the solar distillation system (Sing, 2013).

The result of basin shape (absorber shape) was studied in the research groups of the authors (Gawande and Bhuyar, 2013; Nagarajan and Radhakrishnan, 2015; Alawee et al., 2021). The tested basin shapes were flat, concave, convex, and double basin. Here, it was concluded that a convex-shaped basin can have higher efficiency. The influence of water level on the efficiency of the still was analysed in some previous works. They all agreed that lower water depth can increase the efficiency of solar stills (Al-Garni et al., 2011; Jaimes, Arroyo, and Jaimes, 2017; Nagarajan and Radhakrishnan, 2015; Rajamanickam and Ragupathy, 2012).

The result of wind speed was studied in previous works (Badran, 2011; Afrand and Karimipour, 2017). The authors of the first work said that wind speed can enhance efficiency, while the other reported that wind speed had no significant effect on fresh water production. The solar still efficiency can also be improved by adding an external heat source.

The result of external heat sources was studied in many researchers (Thakur and Ali, 2015; Al_qasaab M.R. et al.,2021; Hassan, 2020; Anand C.S. et al., 2019, Fathy, Hassan, and Ahmed, 2018; Rashak, Ala'a, Khanfoos, 2016; Kalbande, Khambalkar, and Priyankanayak, 2016). In their studies, the solar still was connected to an external heat source such as a flat plate, parabolic, and evacuated tube collector. All of the authors concluded that the cooperation of external heat sources can enhance the efficiency of solar stills. In this study, Sonker, V.K. et al. investigated a solar distillation system applying different phase-changing materials saved in a cylinder (Sonker, V.K. et al., 2019). It was found that lauric acid has better performance than the two other phase change materials (PCMs).

Concerning the performance of different collector shapes, many researchers have made many attempts to determine the incline performance of glass covers of single type, double type, pyramid type, spherical type, and hemispherical type. Comparing the pyramid shape with the two other single and double slopes, the pyramid solar still showed the largest productivity. According to the investigation of some researchers, the performance of a hemispherical shape collector is slightly lower than that of a flat plate collector (Ahmed, Alshutal, and Ibrahim, 2014; Arunkumar et al., 2012; Hashim, Al-Asadi, and Alramdhan, 2010; Anand C.S. et al., 2019; Pareshi P.R. et al., 2019; Al_Qasaab M.R. et al., 2021).

In addition to experiments, Computational Fluid Dynamics (CFD) also plays a vital role in studies for validating experimental results and extending analysis with variations of multiple parameters and designs, which are not easy to find out in an experimental way (Kabeel, El-Said, and Abdulaziz, 2019). CFD numerical simulations on the performance of solar distillation systems were investigated in previous works (Keshtkar Eslami and Jafarpur, 2020; Gnanavel, Saravanan, and Chandrasekaran, 2021; Al-Madhhachi and Smaisim, 2021).

Terres et al. (2022) applied CFD simulation for the analysis of velocity and density distribution in a pyramid-type solar distillation system. The results indicate that the highest maximum temperature happened at the basin (tray). The authors concluded that CFD can give a better understanding of still operation, and it is a verification for experimental observations. El-Sebaey et al. (2020) used CFD for the modelling of temperature distribution, vaporization, and velocity of vapour in conventional basin-type solar stills. Their CFD results showed an adequate arrangement with the experimentally measured data. Then, Sonawane et al. (2022) analysed how basin absorber materials affect the fulfilment of a single-slope solar still using CFD. The authors solved the energy equation and momentum equation to obtain the temperature and velocity distribution.

All the previous studies focused on how basin shape, water level, wind velocity, external heat source, and different collector shapes affected distilled output. Most previous studies applied CFD simulation to predict the operation conditions of single-slope solar stills. Also, other authors have worked on CFD simulations for square pyramid solar stills. Since it can give greater productivity compared to the other shapes, the pyramid shape of the solar

still was selected for this study. Therefore, the aim of this work is to analyse absorber temperature, water temperature, and glass cover temperature in a pyramid solar still by theory, CFD simulation, and experimentation because temperature distribution is the main factor in enhancing the pure water output of the solar still.

## METHODOLOGY

### Theoretical Temperature Analysis for Solar Stills

Figure. 2 presents a typical pyramid solar-energy-based still in various heat transfer modes. It was based on the coefficients of internal heat and mass transfer in the solar still for radiation, evaporation, and convection. The heat internal transfer coefficient directly deals with the distilled output efficiency. These heat transfer modes can be based on the calculation of the temperature profile of the glass cover, water, basin absorber, and pure water productivity by using the energy balance equation. The energy conversation equation of the system parts temperature of the solar still is as follow:

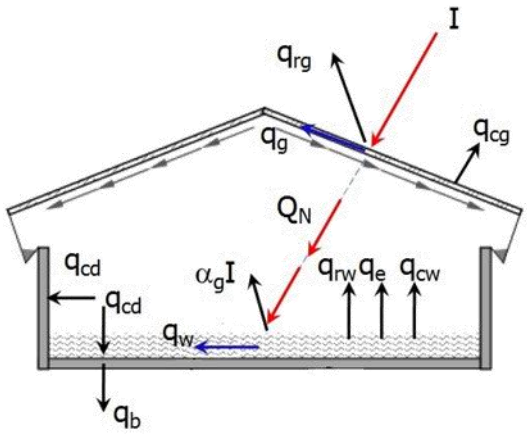


Figure 2. Typical pyramid solar-energy-based water distillation system

$$m_g C_{pg} \frac{dT_g}{dt} = \alpha_g I A_{gp} + A_g [q_{rw} + q_{cw} + q_e - (q_{rg} + q_{cg})] \quad (1)$$

$$m_w C_{pw} = \frac{dT_w}{dt} A_w (I\tau_g \alpha_w - q_{rw} - q_{cw} - q_e - q_{cd}) \quad (2)$$

$$m_b C_{pb} \frac{dT_b}{dt} = A_b (I\tau_g \tau_w \alpha_b - q_{cd} - q_b) \quad (3)$$

Where, I is direct heat flux ($W/m^2$), $q_{rg}$ is radiation at glass ($W/m^2$), $q_{cg}$ is convection at glass, $q_g$ is heat stored at glass ($W/m^2$), $Q_N$ is total heat ($W/m^2$), $q_w$ is heat stored in water ($W/m^2$), $q_{rw}$ is the water heat radiation ($W/m^2$), $q_{cw}$ describes heat convection by water ($W/m^2$), $q_e$ is evaporating heat loss ($W/m^2$), $q_{cd}$ is conducting heat loss ($W/m^2$),$\alpha$ means the coefficient of the absorption, $\tau$ express the coefficient of transmittance, and $q_b$ reveals heat loss to surrounding ($W/m^2$).

Convection, evaporation, and radiation heat transfer from the solar water distillation are calculated according to the following equations:

$$q_{cw} = 0.884[(T_w - T_g) + \frac{(P_w - P_g)(T_w + 273)}{268.9\times10^3 - P_w}](T_w - T_g) \quad (4)$$

$$q_{ew} = 16.276\times10^{-3}\times q_{cw}\frac{(P_w - P_g)}{T_w - T_g} \quad (5)$$

$$q_{rw} = \varepsilon_w\sigma[(T_w+273)^4 - (T_g-273)^4] \quad (6)$$

Where, $p_w$ and $p_g$ are the partial pressure of water vapor in the basin water and the glass in Pascal, and $T_w$ and $T_g$ reveal water and glass temperature, $\sigma$ reveals the Stefan-Boltzman constant ($5.67\times 10^{-8}$ $JK^{-4}m^{-2}$) and $\varepsilon_w$ is the emission of water.

The convection and radiation heat transfer of the glass can be calculated by Eqs. [7-8].

$$q_{cg} = (5.7 + 3.8\, V_{wind})(T_g - T_a) \quad (7)$$

$$q_{rg} = \varepsilon_g\sigma[(T_g+273)^4 - (T_a+273)^4] \quad (8)$$

Where, $\varepsilon_g$ is the glass emission. Then, the convection heat transfer from the still water to the absorbing surface of the basin ($W/m^2$) can be solved by the following formula.

$$q_{cd} = h_{wb}(T_w - T_b) \quad (9)$$

The convection heat transfer from the basin can be obtained by Eqs. [10].

$$q_b = h_{ba}(T_b - T_a) \quad (10)$$

$$\frac{1}{h_{ba}} = \frac{\delta_{in}}{k_{in}} + \frac{1}{h_a} \quad (11)$$

Where, $h_{wb}$ is the water heat transfer coefficient and $h_{ba}$ is the coefficient of heat transfer from the basin to the air.

**Governing Equations**

In solar still simulations, the targeted parameter is temperature distribution. Thus, energy equation, continuity equation, and momentum equation were solved in this work. Therefore, the main governing equations are described in the following equations.

Continuity equation:

$$\frac{\partial\rho}{\partial t} + \nabla.(\rho\vec{v}) = 0 \quad (12)$$

Momentum equation:

$$\frac{\partial(\rho\vec{v})}{\partial t} + \nabla.(\rho\vec{v}\vec{v}) = -\nabla p + \nabla.(\vec{\tau}) + \rho\vec{g} \quad (13)$$

Energy Equation

$$\frac{\partial(\rho E)}{\partial t} + \nabla.(\vec{v}(\rho E + p)) = \nabla.(k_{eff}\nabla T) + S_h + S_L \quad (14)$$

Where, ρ means density, T describes temperature, E is energy, v means velocity, g describes gravitational acceleration, $k_{eff}$ is effective thermal conductivity, $S_h$ is radiant energy, and $S_L$ is evaporation heat.

After obtaining the average water and glass temperature in a solar energy-based solar still at any local hour, the pure water productivity is calculated by using the following equations.

$$m_{the} = 16.273\times10^{3}h_{cw}\left(\frac{P_w - P_g}{L}\right) \quad (15)$$

$$L=2.569\times10^{5}(647.3-Tw)^{0.38} \quad (16)$$

$$P_w = \exp\left(25.317-\frac{5144}{273.15+T_w}\right) \quad (17)$$

$$P_g = \exp\left(25.317-\frac{5144}{273.15+T_g}\right) \quad (18)$$

Where, $m_{the}$ means distillation water flow rate, L describes vaporized, and $h_{cw}$ can be seen in Eq [4].

Temperature distribution and fresh water productivity were calculated by using the input system parameters in MATLAB software. Table.1 shows the input system parameters and calculated parameters of the pyramid solar water distillation system [29].

Table 1. System Specification Parameter and Simulation Parameters

| System parameters | Symbols | Specifications |
|---|---|---|
| Total area of glass cover ($m^2$) | $A_g$ | 1.314 |
| Total area of water ($m^2$) | $A_w$ | 0.9776 |
| Total area of basin ($m^2$) | $A_b$ | 0.9776 |
| Glass's absorption coefficient | $\alpha_g$ | 0.05 |
| Water's absorption coefficient | $\alpha_w$ | 0.05 |
| Basin's absorption coefficient | $\alpha_b$ | 0.9 |
| Glass's transmitting coefficient | $\tau_g$ | 0.9 |
| Water's transmitting coefficient | $\tau_w$ | 0.95 |
| Basin's transmitting coefficient | $\tau_b$ | 0.00 |
| Basin wall thickness (m) | $\delta_{in}$ | 0.02 |
| Basin thermal conductivity (W/mK) | $k_{in}$ | 43 |
| Convective heat transfer coefficient of water ($W/m^2K$) | $h_{wb}$ | 50 |
| Convective heat transfer coefficient of air ($W/m^2K$) | $h_{ba}$ | 45 |
| Specific heat capacity of glass (J/kg) | $C_{pg}$ | 649 |
| Specific capacity of water (J/kg) | $C_{pw}$ | 4187 |
| Specific capacity of basin (J/kg) | $C_{pb}$ | 600 |

**Experimental Setup**

The experimental pyramid solar still set-up was located as shown in Figure.3 at the Department of Mechanical Engineering, Mandalay Technological University, Myanmar, where maximum solar heat flux and water supply are readily available.

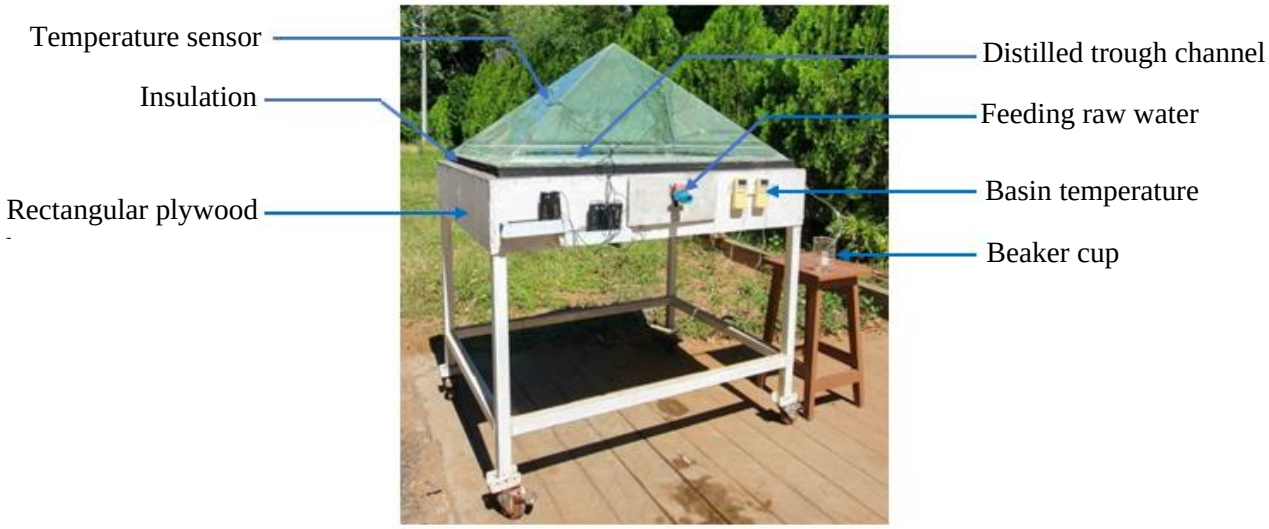


Figure 3. Experimental setup of pyramid solar still

The north latitude is 21.996°, and the east longitudinal is 96.1°. Firstly, the pyramid solar still was made up of steel and plywood. The glass cover thickness is 5mm. The tilted angle of the glass covers was set at 45°. The glass cover total area is 1.314 $m^2$ and the height is 425 mm. The polystyrene foam insulation material is 38.1 mm, which is used to reduce heat loss from the system. The total width of the solar still is 896 mm, and length of the solar still is 1210 mm. The total height from the basin base to the pyramid tip is 625 mm.

The solar still basin was made of a mild steel sheet rectangular box. The sheet metal thickness is 3mm. The sheet metal rectangular bin was set into the ply-wood bin, which is constructed with a 5 mm-thick ply-wood plate. The polystyrene insulation board was inserted between the bin and the basin to prevent heat loss from the bottom and side walls of the solar still. The glass cover on the edges is fitted tightly to prevent air from entering the basin. A distilled trough channel was used for the collection of the distilled water, which is drained into a beaker that is placed outside of the basin. An inlet PVC pipe was fitted to the back side wall of the solar still for filling tap water. The appropriate four-legged iron stand was used for the proposed solar still. Caster wheels were attached at the ends of four legs for smooth movement and direction of the solar still. The inner absorber was painted in black colour in experimental tests.

In the experiments, the solar power meter was applied to test the hourly solar radiation of the solar still. The digital thermometers (DS1) and the laser temperature sensor (RayTek ITC-45) were applied to measure the temperature of the basin, water, and glass cover in the solar still. The beaker cup measured the amount of fresh water productivity. Two temperature sensors were placed at the base of the vessel surface to measure the vessel temperature. The total of eight temperature sensors was used for measuring the glass temperature. Four temperature sensors were placed on the outer surfaces, and another four thermometer temperature sensors were used on the glass-covered inner surfaces.

The measuring procedure in the experimental test of the pyramid solar still is as follows: Firstly, the working fluid (tap water) was filled in the vessel to obtain the required amount of water depth. The depth of the water was set at 1.0 cm. Secondly; all temperature sensors were adjusted to be at the same level at the environmental temperature around 7:00 a.m in the morning. The environmental temperature was 26 °C. Thirdly, the measurements of solar heat flux and each temperature of the basin, water, and glass were made starting at 9:00 a.m in the morning and continuing every hour. Then, the fresh water produced by the solar still was collected in the beaker cup and measured every hour

to obtain hourly production, and all result data were accumulated until the end of the experiment. At the end of the day, the total volume of daily output fresh water was obtained.

## NUMERICAL SIMULATION APPROACH

There are five steps in CFD numerical simulation: creating geometry, meshing to geometry, boundary conditions, solver setting, and results. In this investigation, numerical simulation was done for temperature analysis in a pyramid-shaped solar system using ANSYS FLUENT software.

### Geometry and Mesh Model

The numerical procedure of the solar still in FLUENT is shown in Figure.4. The numerical dimensions of the pyramid solar still are the same as in the experimental design. The three-dimensional geometry model for the pyramid solar distillation system was created in GAMBIT and imported to ANSYS software. Figure.5 presents the 3D geometry of the pyramid-shaped solar still. Figure.6 describes the structure design of the mesh generation; the mesh are tetrahedral elements. There are a total of 30214 elements and 6185 nodes. The maximum mesh size is 0.001571m.

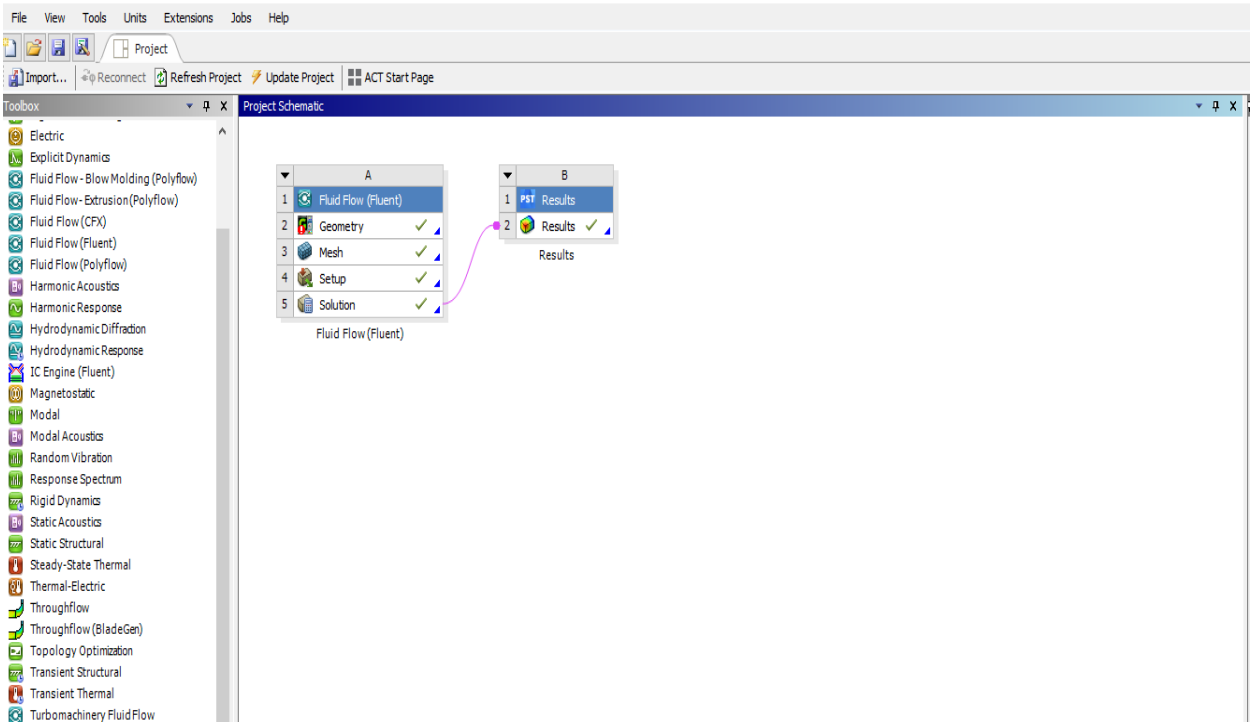


Figure 4. Numerical process for the analysis of the pyramid distillation system

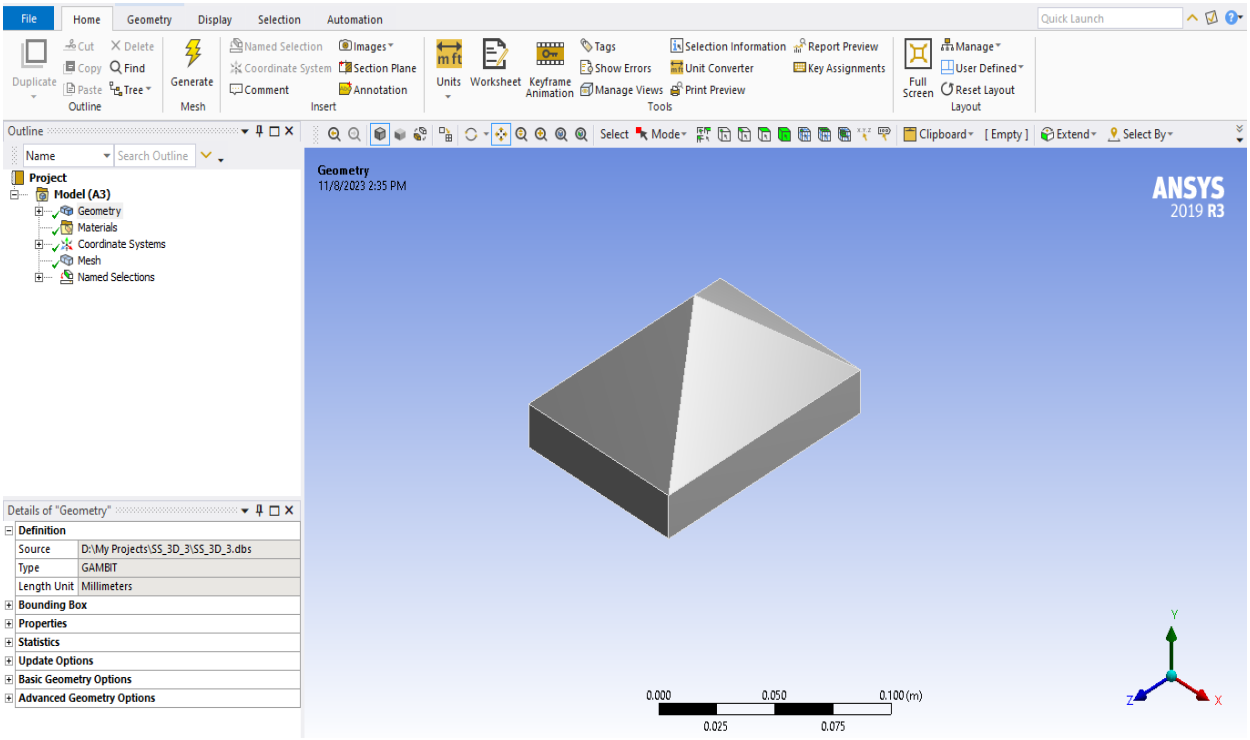


Figure 5. Three-dimensional shape of the pyramid type distillation system

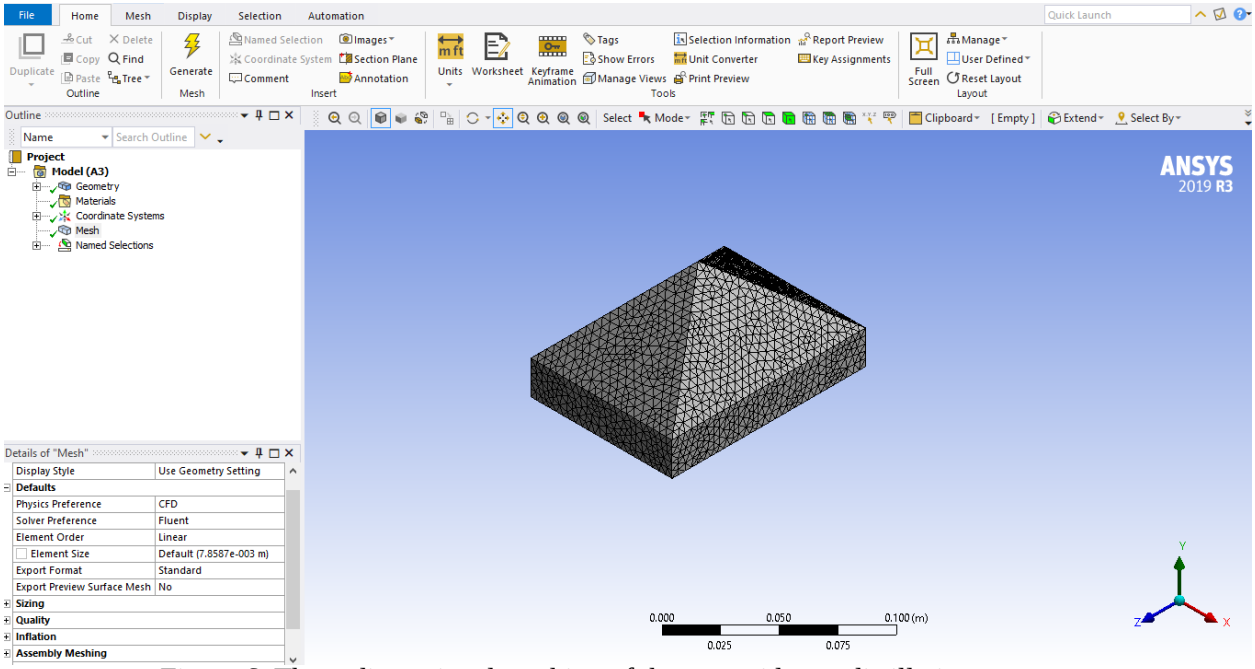


Figure 6. Three-dimensional meshing of the pyramid type distillation system

**Boundary Conditions and Assumptions**

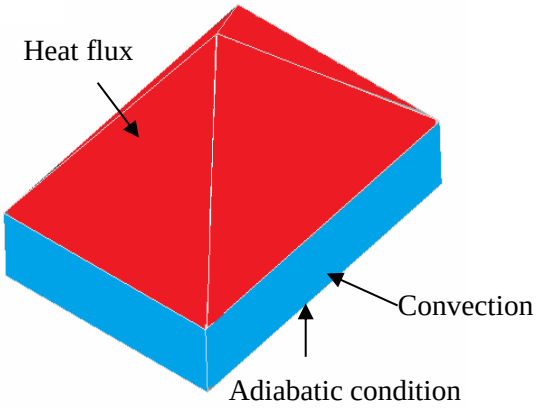


Figure 7. Boundary conditions of computational domain

The boundary conditions and solver system of the solar still in ANSYS FLUENT are described in Table 2. In this section, the solar heat flux of the solar still is the main factor in the pyramid solar distillation systems. First, an incident of solar radiation falls onto the glass cover due to the absorptivity and transmissivity of the glass. The basin absorber absorbed the radiation, which causes higher water temperatures. The computational boundary conditions are shown in Figure.7. In the simulation, it is assumed that there are no heat losses from the absorber plate. Then, a constant solar heat flux was applied to the outer glass surfaces during the simulation period. Then convection conditions were applied to the side surface of the solar still.

All the boundary conditions specified the mesh model to solve the continuity and momentum equations. The density of the fluid (water) is assumed to vary linearly with the temperature. The initial temperature of water was set at 300°K, which is measured value in the experimental test. The water level was set to a constant of 1.0 cm, as in the experiments. Table.3 expresses the following solver condition for the multiphase simulation parameter of the pyramid solar still.

Table 2. Boundary conditions of the pyramid solar still

| Domain | Location | Types | Thermal condition | Description |
|---|---|---|---|---|
| Solid | absorber | wall | Adiabatic condition | Opaque |
| | wall | wall | Convection ($3W/m^2K$) | Opaque |
| | Glass plate -1 | wall | Heat flux of fixed wall | Semi-transparence |
| | Glass plate -2 | wall | Heat flux of fixed wall | Semi-transparence |
| | Glass plate -3 | wall | Heat flux of fixed wall | Semi-transparence |
| | Glass plate -4 | wall | Heat flux of fixed wall | Semi-transparence |

Table 3. The solver condition of the multiphase simulation parameter of the pyramid solar still

| Function | | Specification |
|---|---|---|
| Operation conditions | Operating pressure | 1.01 bar |
| | Gravity | -9.81, Z-Direction |
| | Operating temperature | 288.16K |
| | Space | 3D |
| Solver setting | Viscous model | Unsteady, first order implicit |
| | Multiphase model | Standard, k-epsilon turbulence model with wall treatment |
| | | Thermal effects and viscous heating |

| | | | |
|---|---|---|---|
| | Radiation | Rosseland radiation model, solar loading and solar ray tracing<br>Inputs: Latitude 21.98° N and Longitude 96.1°E<br>Day: 23 | Time: 13:00 |
| Material Properties | Solid | Glass, GI sheet, and wood | Thermo-physical properties: density, thermal and conductivity and specific heat capacity of the materials |
| | Fluid | Air, water liquid, and water vapour | |
| Phases | Three phases | Primary phase<br>Secondary Phase | Air,<br>Water liquid, Water vapour |

## RESULTS AND DISCUSSIONS

The theoretical, numerical, and experimental results of the receiving solar heat flux, temperature distribution of the absorber, glass cover, water inside the pyramid solar still, and pure water output rate are presented and discussed as following.

Solar Heat Flux

Figure.8 shows the comparison of the hourly solar heat flux measured in the experiment and theoretical values at different local times. The results of the solar heat flux were noted from 9 a.m to 5 p.m in the experiment. The maximum heat flux occurred at 811.36 W/m$^2$ in theory and at 799.32 W/m$^2$ in the experiment at noon, and they were verified with each other. It can be noted that the solar heat flux increased until it reached the maximum peak point at the local time of noon. After the peak at noon, the declination is steeper in the afternoon compared to the trend in the morning. Increasing solar heat flux made a significant increase in freshwater production rate because the solar heat flux is mainly important for freshwater productivity.

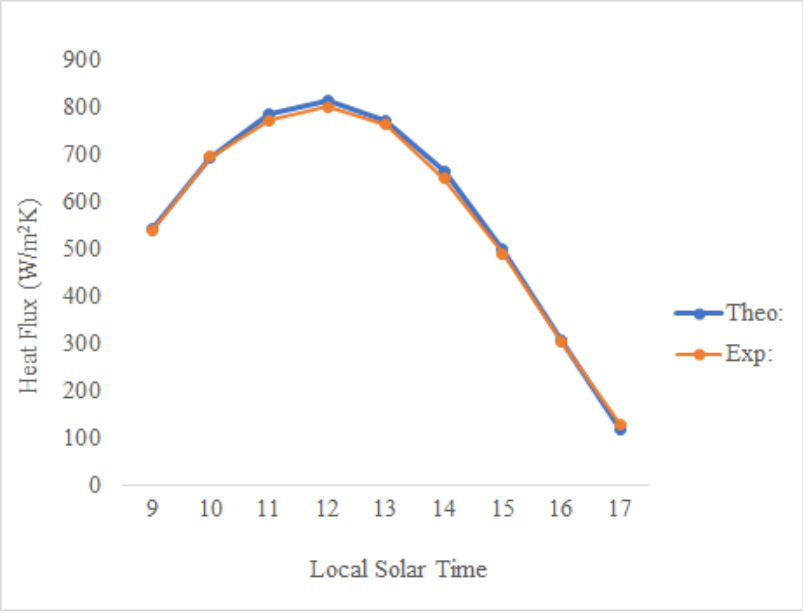


Figure 8. Solar heat flux at various local solar hours

**Comparison of Temperature Distribution in Pyramid Solar Still**

In the following Figure 9(a)-9(c), the numerical results of the vessel temperature distribution in the still at local times of 9 a.m, 1p.m, and 3 p.m are shown. The maximum temperature occurred at about 316.42 K at 9 a.m, while about 331.63 K was obtained at 1:00 p.m and around 326.68 K was attained at 3p.m.

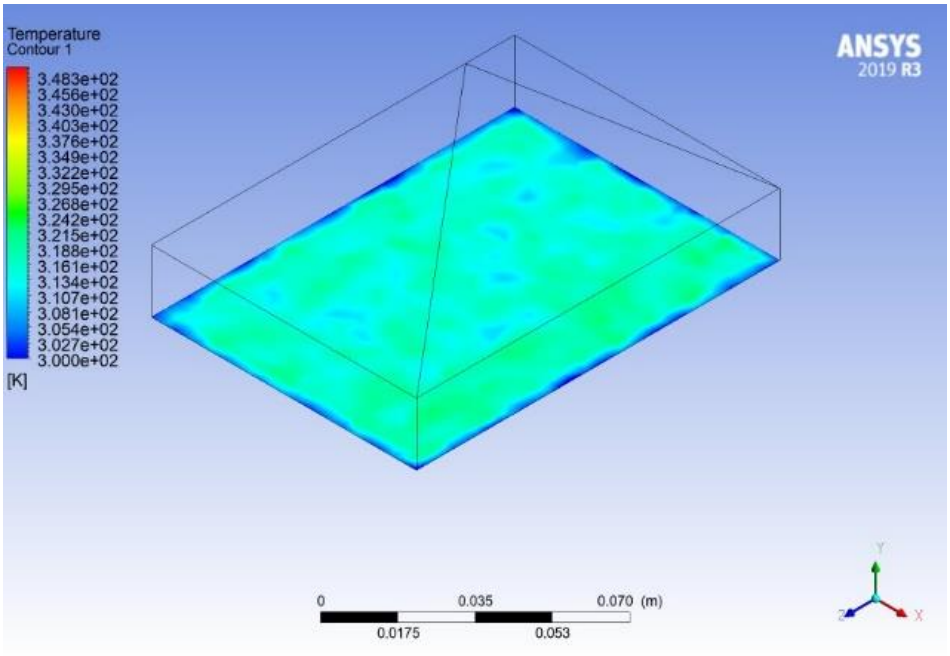


Figure 9. (a) Basin temperature distribution at 9:00 a.m

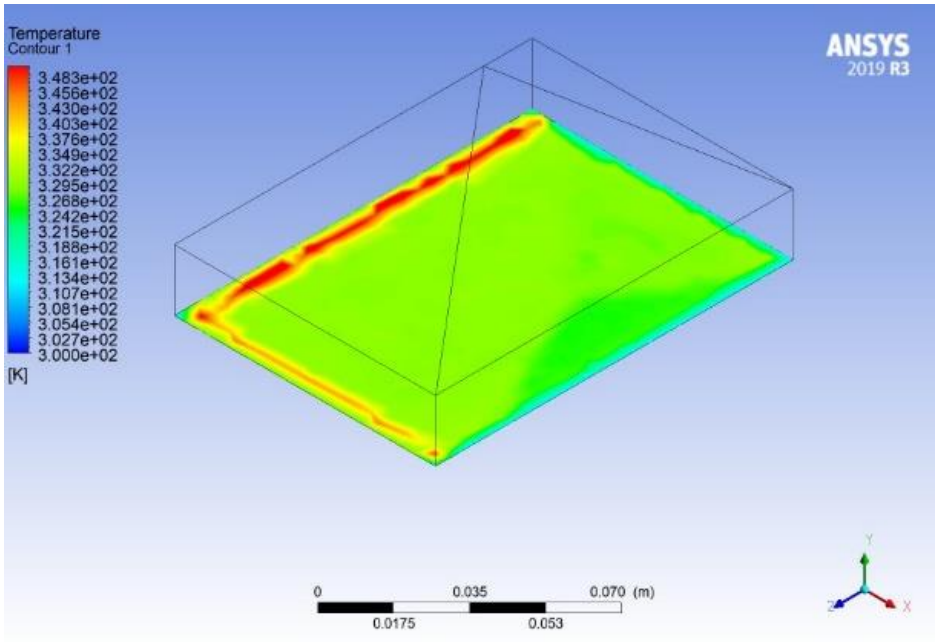


Figure 9. (b) Basin temperature distribution at 1:00 p.m

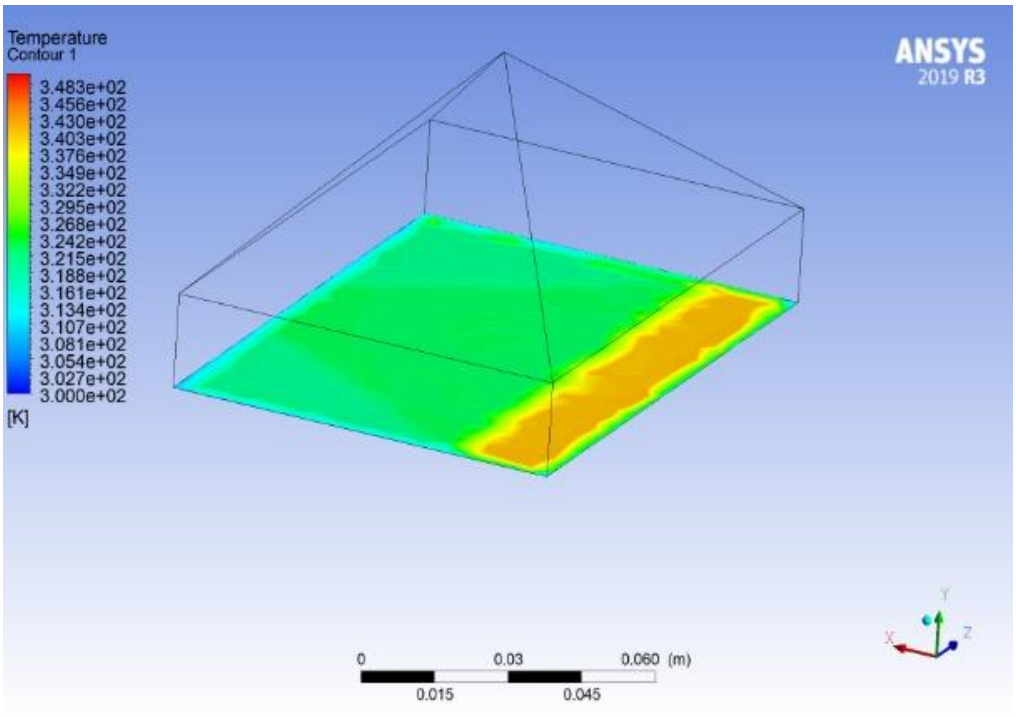


Figure 9. (c)Basin temperature distribution at 3:00 p.m

Figure. 10(a)-10(c) show the water temperature distributions in a pyramid-shaped solar still in the morning, afternoon, and evening times. It shows that the water and absorber temperature (basin temperature) are nearly the same at the absorber wall, and the temperatures at 9 a.m, 1 p.m, and 3 p.m are about 315 K, 331 K, and 312 K respectively.

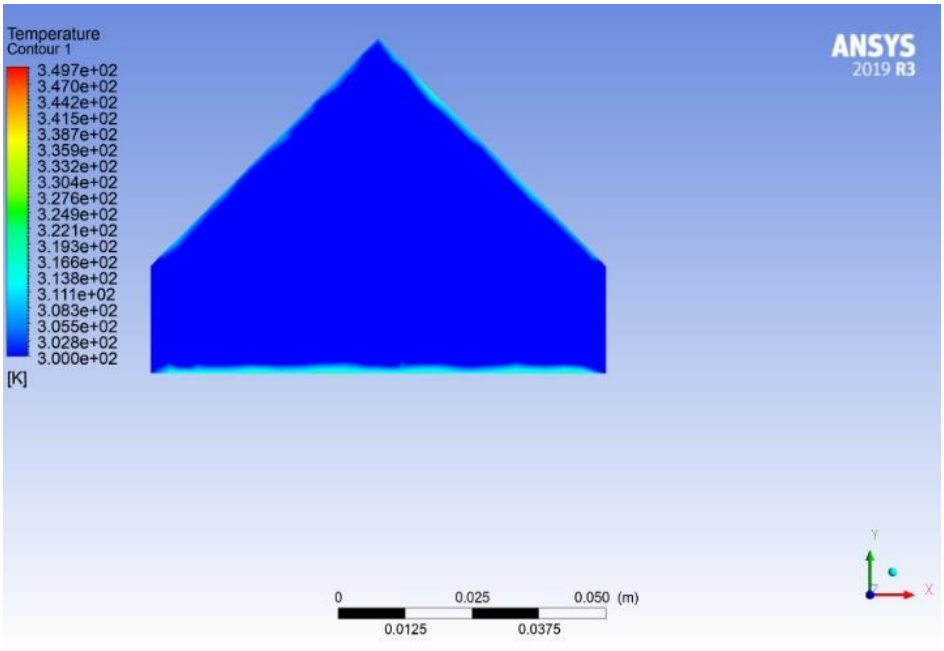


Figure 10. (a) Water temperature distributions of pyramid type at 9:00 a.m

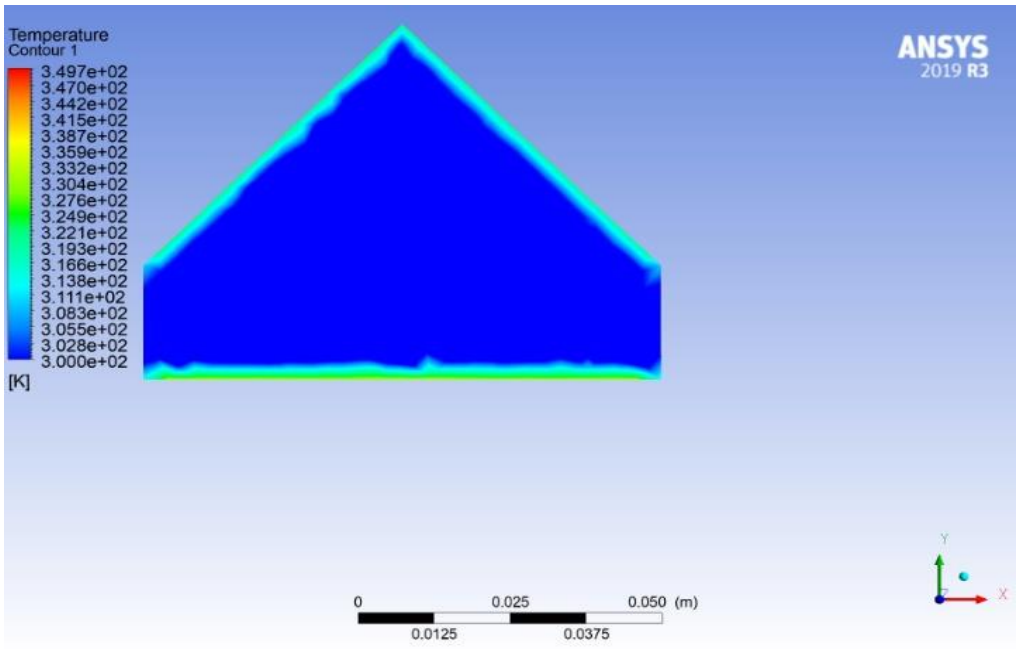


Figure 10. (b) Water temperature distributions of pyramid type at 1:00 p.m

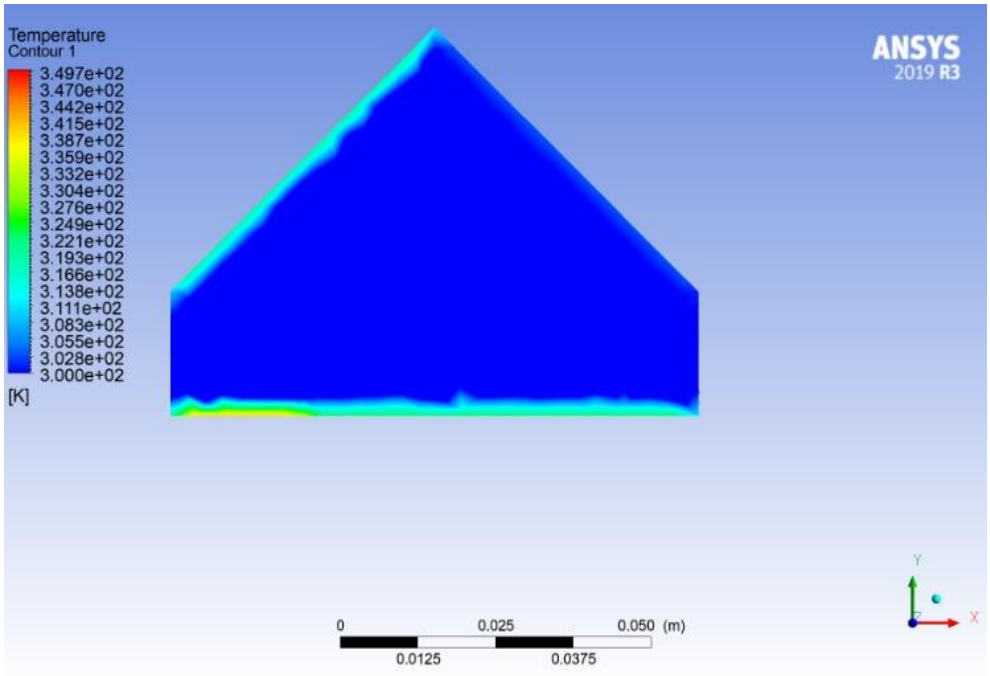


Figure 10. (c) Water temperature distributions of pyramid solar still at 3:00 p.m

The temperature distribution of the glass cover of the pyramid solar still at 9 a.m, 1 p.m, and 3 p.m are shown in the following Figures 11(a)-11(c). It found that the glass topping attained about 309.75 K at 9 a.m. At the same time, nearly 321 K was occurred at 1p.m and around 312.71 K was obtained at 3 p.m.

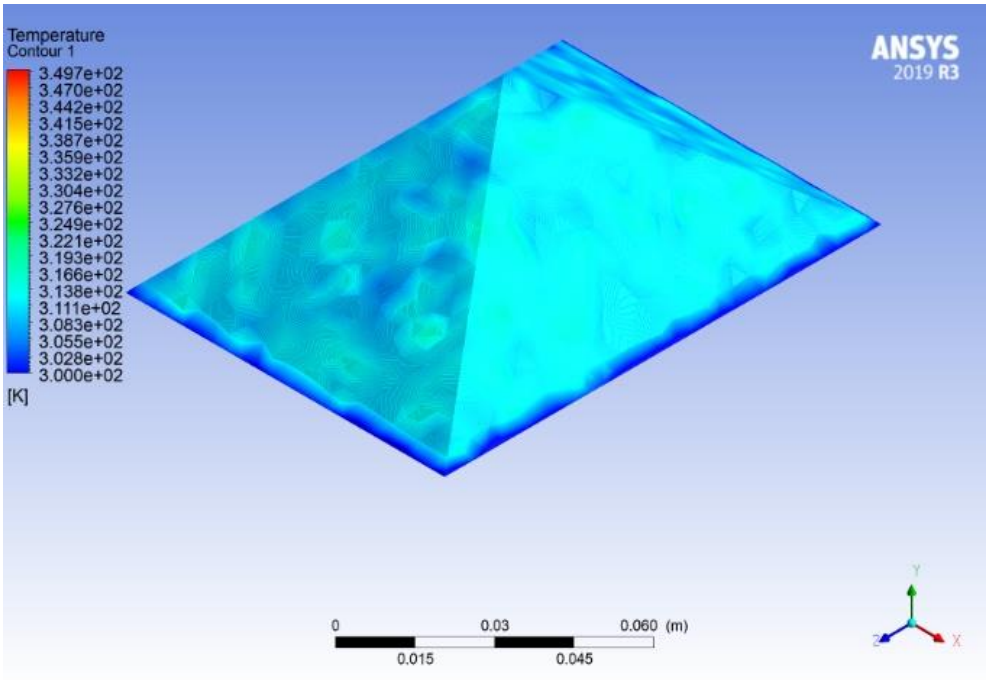


Figure 11. (a) Glass cover temperature distributions of pyramid solar still at 9:00 a.m

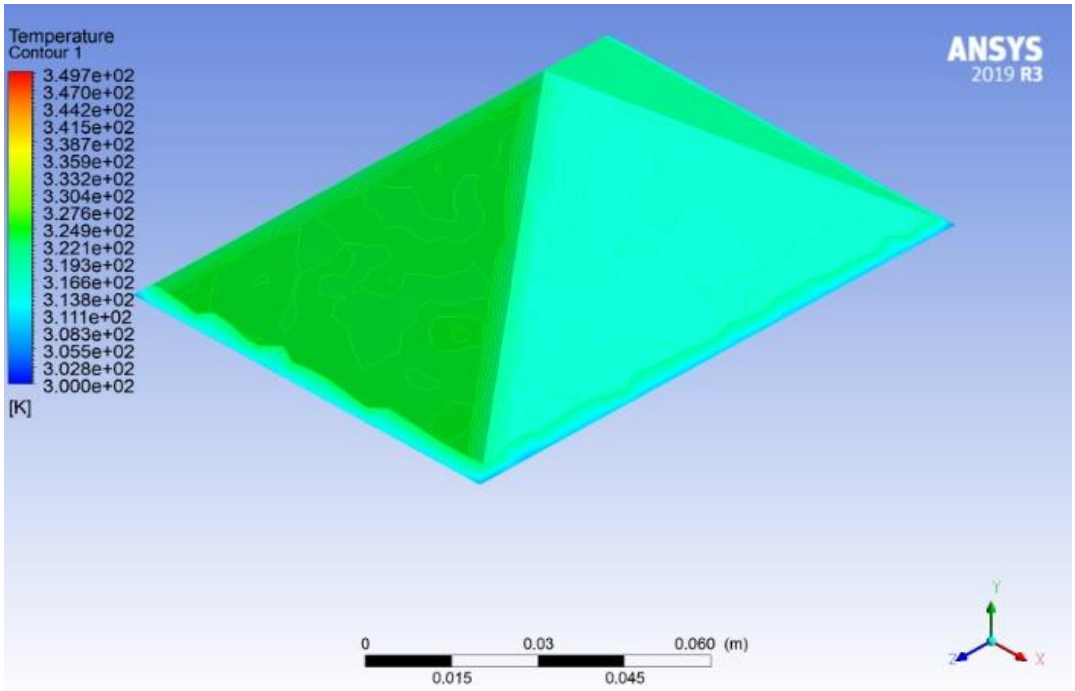


Figure 11. (b) Glass cover temperature distributions of pyramid solar still at 1:00 p.m

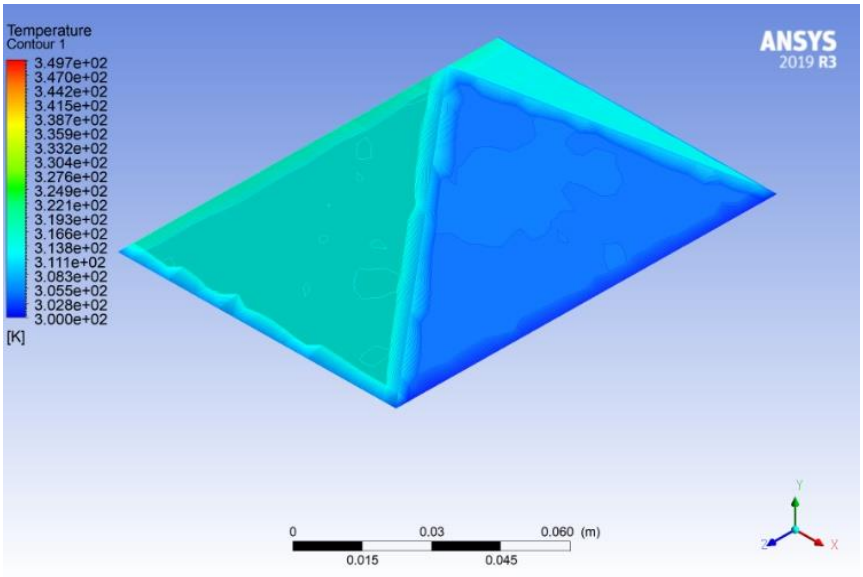


Figure 11. (c) Glass cover temperature distribution of pyramid solar still at 3:00 p.m

The CFD analysis was conducted to achieve temperature analytical results for the pyramid solar still. The red colour shows the maximum temperature, which was found at the basin absorber plate. At the same time, the blue colour means the minimum temperature that was met at the glass cover. It observes that the basin absorber temperature is highest, the water temperature is second highest, and glass cover temperature is lowest. The maximum temperature of water in the solar still was 73°C at 1p.m, and the minimum temperature occurred at 43°C at 9 a.m.

Figures 12-14 show the comparison of the temperature distribution of the absorber, water, and glass cover of the solar still among the theoretical, numerical, and experimental results. It can be observed that the theoretical and simulation results were obtained with good accuracy compared with the experimental data. Although the readings of the results are slightly different, the trends have similar patterns. The basin temperature distribution is similar to trends in the water temperature distribution due to the solar intensity observed by the basin's black surface during daylight. The heat from the absorber plate transfers to the water by convection. For glass temperature, the profiles of theoretical and CFD simulation outputs are slightly different from the experimental results because only solar radiation mode was set in the simulation model and did not consider other environmental effects, such as the wind effect, as in the experiment. Also, the trend of the solar heat flux is followed by the hourly temperature distribution.

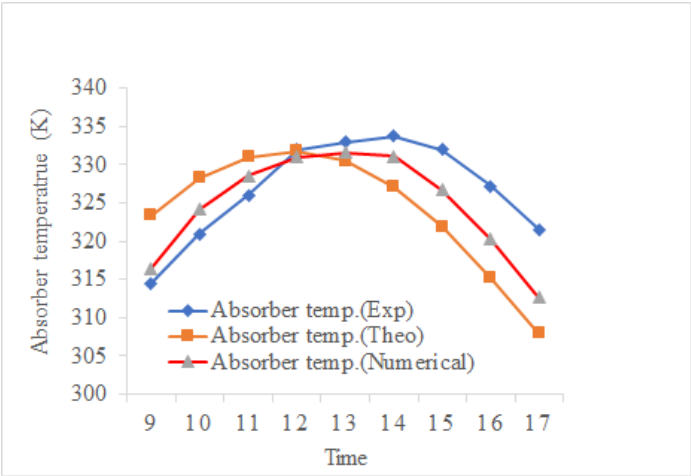


Figure 12. Temperature distribution of basin absorber in solar still

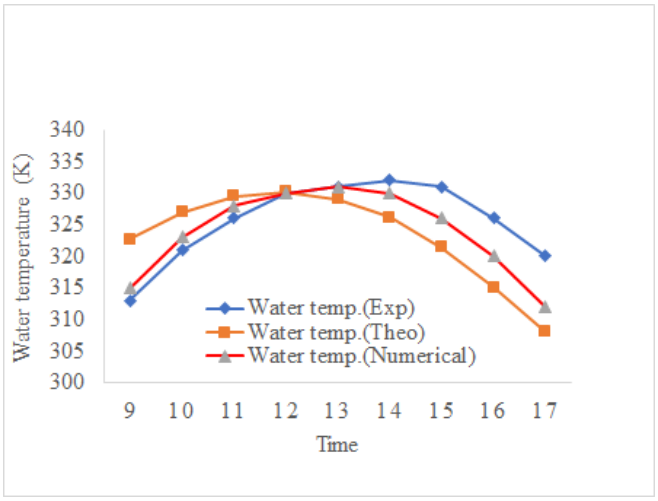


Figure 13. Temperature distribution of water in solar still

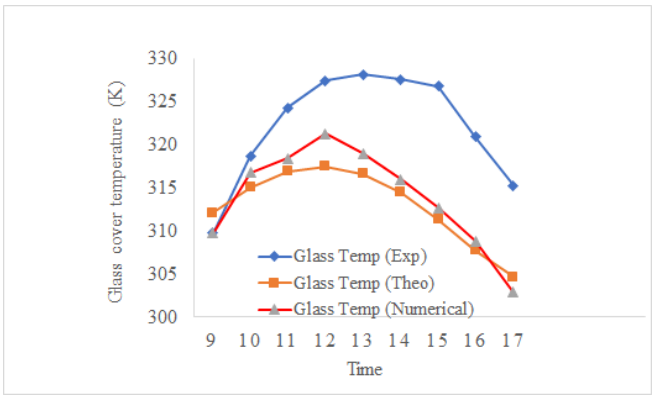


Figure 14. Temperature distribution of glass cover in solar still

Figure.15 shows the theoretical, CFD simulation, and experimental results of freshwater productivity at different times. From all the results, it can be found that the freshwater productivity curves have a similar trend, which is verifying each other. The maximum freshwater productivity was obtained in the afternoon. This is because of the higher solar intensity at this time. The heat losses from the basin to the surrounding area was reduced by the high solar intensity. It can be seen that the maximum theoretical result of the freshwater productivity was 335.5 ml/hr, while the CFD simulation result was 357.4 ml/hr and the maximum production rate of 437.5 ml/hr was in the experimental test. Thus, the result explains that the maximum peak point of freshwater productivity is not consistent with the peak point of solar heat flux due to the time taken for evocation.

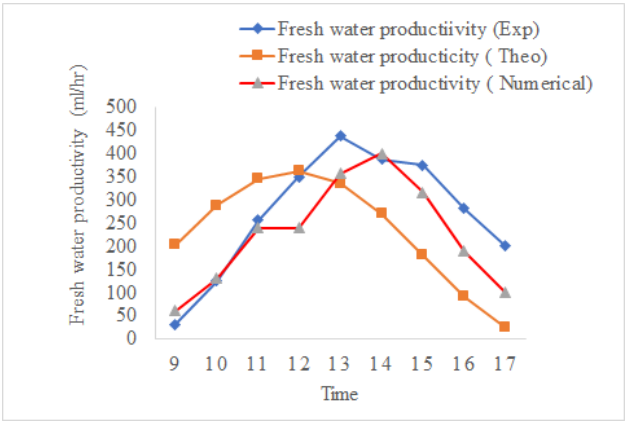


Figure 15. Fresh water productivity in solar still

## CONCLUSION

In this study, the temperature distributions of absorber, water, glass, and freshwater productivity in pyramid solar stills were investigated using theoretical, CFD simulation, and experimental tests. The tilted glass cover of 45° was constructed in a pyramid solar still. The thermal analysis was conducted in MATLAB software, and CFD simulation was used on ANSYS Fluent. And also, the tap water level of 1cm was filled in the vessel, which floor was covered with black absorber. In the experimental operation, the daily system temperature profile, thermal radiation, and fresh water productivity were collected at Mandalay Technological University (MTU), Mandalay, Myanmar, on 23rd April, 2022. The maximum operating water temperature of 330 K was obtained theoretically, and 331 K was received in the CFD simulation, while the largest experimental water temperature was 332 K. And also, the maximum fresh water production in the theoretical, CFD simulation, and experiments were 335.8 ml/hr, 399.5 ml/hr and 437.5 ml/hr respectively, at noon. It can be noted that daily distilled output increases with a higher operating water temperature and condensing plane for distillation. Therefore, a greater temperature difference between the evaporation and condensing surfaces can produce more daily distilled water. Above all, the temperature distribution results of the absorber, water, glass cover, and fresh water productivity are reasonable compared to theoretical, CFD simulation, and experimental outputs.

## REFERENCES

Afrand, M. & Karimipour, A. (2017). Theoretical analysis of various climatic parameter effects on performance of a basin solar still. *Journal of Power Technologies*, 97(1), 44-51.

Ahmed, H.M., Alshutal, F.S. & Ibrahim, G., (2014). Impact of different configurations on solar still productivity. *Journal of Advanced Science and Engineering Research*, 3(2), 118-126.

Alawee, W.H., Mohammed, S.H., Dhahad, H.A, Essac, F.A, Omarac, Z.M & Abdullah, A.S. (2021). Performance analysis of a double-slope solar still with elevated basin —comprehensive study. *Desalination and Water Treatment*, 223, 13-25.

Al-Garni, A.Z., Kassem, A.H., Saeed, F. & Ahmed, F., (2011). Effect of glass slope angle and water depth on productivity of double slope solar still. *J SCI IND*, 70(10), 884-890.

Al-Madhhachi, H. & Smaisim, G.F. (2021). Experimental and numerical investigations with environmental impacts of affordable square pyramid solar still. *Solar Energy*, 216, 303-314.

Al_qasaab, M.R., Abed, A.Q., & Abd Al-wahid, W.A. (2021). Enhancement the solar distiller water by using parabolic dish collector with single slope solar still. *Journal of Thermal Engineering*, 7(4), 1000-1015.

Anand, C.S., Suresh, J., & Sreekumar, P.C. (2019). Desalination of Water Using Double Slope Double Basin Solar Still Coupled with Evacuated Tubes. *International Journal of Innovative Technology and Exploring Engineering*, 8(6s2), 127-130.

Arunkumar, T., Vinothkumar, K., Ahsan, A., Jayaprakash, R., & Kumar, S. (2012). Experimental study on various solar still designs. *ISRN Renewable Energy*.

Badran, O. (2011). Theoretical analysis of solar distillation using active solar still. *Int. J. of Thermal & Environmental Engineering*, 3(2), 113-120.

Fathy, M., Hassan, H., & Ahmed, M.S. (2018). Experimental study on the effect of coupling parabolic trough collector with double slope solar still on its performance. *Solar Energy*, 163, 54-61.

Gawande, J.S. & Bhuyar, L.B. (2013). Effect of shape of the absorber surface on the performance of stepped type solar still. Energy and Power Engineering, 5(8), 489-497.

Gnanavel, C., Saravanan, R., & Chandrasekaran, M. (2021). CFD analysis of solar still with PCM. Materials Today: *Proceedings*, 37, 694-700.

Hassan, H. *(*2020). Comparing the performance of passive and active double and single slope solar stills incorporated with parabolic trough collector via energy, exergy and productivity. *Renewable Energy*, 148,.437-450.

Hashim, A. Y., Al-Asadi, J. M., & Alramdhan, W. T. (2010). An attempt to solar still productivity optimization: Solar still shape, glass cover inclination, and inner surface area of a single basin solar still, optimization. *Basrah Journal of Science*, 28(1A English), 39-48.

Jaimes, A.S., Arroyo, E.H., & Jaimes, Z.Y.R., *(*2017). Experimental evaluation of a single slope solar still. *Tecciencia*, 12(22), 63-71.

Kabeel, A.E., El-Said, E.M.S., & Abdulaziz, M. (2019). Computational fluid dynamic as a tool for solar still performance analysis and design development: a review. *Desalination Water Treat*, 159, 200-213.

Kalbande, S.R., Khambalkar, V.P., & Priyankanayak, S.D. (2016). Development and Evaluation Solar Still Integrated with Evacuated tubes. *International Journal of Research in Applied*, 4, 99-106.

Keshtkar, M., Eslami, M., & Jafarpur, K. (2020). A novel procedure for transient CFD modeling of basin solar stills: Coupling of species and energy equations. Desalination, 481, 114350.

Nagarajan, B., & Radhakrishnan, R. (Year). Design and Fabrication and Performance Analysis of Concave Basin Pyramid Type Solar Still with Various Parameters. *International Journal of Applied Engineering Research, 10*(15), 12181-12194.

Pareshi, P. R., Dhande, K. K., Bhagat, G., Suvarnkar, V., & Javanjal, V. (2019). Solar Water Distillation System by Using Inclined Double Basin. *International Research Journal of Engineering and Technology, 6*(3), 1310-1313.

Rajamanickam, M. R., & Ragupathy, A. (2012). Influence of water depth on internal heat and mass transfer in a double slope solar still. *Energy Procedia, 14*, 1701-1708.

Rashak, Q. A., Ala'a, A. J., & Khanfoos, H. N. (2016). Improving the productivity of solar still using evacuated tubes. *International Journal of Energy and Environment, 7*(5), 375.

El-Sebaey, M. R., Ellman, A., Hegazy, A., & Ghonim, T. (2020). Experimental analysis and CFD modeling for conventional basin-type solar still. *Energies, 13*(21), 5734.

Singh, N. (2013). Performance analysis of single slope solar stills at different inclination angles: an indoor simulation. *International Journal of Current Engineering and Technology, 3*(2), 677-684.

Sonawane, C., Alrubaie, A. J., Panchal, H., Chamkha, A. J., Jaber, M. M., Oza, A. D., ... Burduhos-Nergis, D. P. (2022). Investigation on the impact of different absorber materials in solar still using CFD simulation—economic and environmental analysis. *Water, 14*(19), 3031.

Sonker, V. K., Chakraborty, J. V., & Sarka, A. B. (2019). Solar distillation using three different phase change materials stored in a copper cylinder. *Energy Report, 5*, 1532-1542.

Terres, H., Chávez, S., Lizardi, A., Lara, A., Morales, J., Rodríguez, R., & Ruiz, C. (2022, September). CFD Applied to the Analysis of the Operation of a Solar Still Pyramidal-type. *Journal of Physics: Conference Series, 2307*(1), 012002.

Tiwari, G. N., Sahota, L. (2017). *Advance Solar Distillation System* (1st ed.). Springer.

Thakur, C., & Ali, R. (2015). Experimental Investigation of Double Sloped Solar Still Coupled with Flat Plate Solar Water Heater. *International Journal on Recent Technologies in Mechanical and Electrical Engineering, 2*(5), 52-55.